Journal of Physiology (2002), **544.2**, *pp.* 549–565
DOI: 10.1113/jphysiol.2002.023267

www.jphysiol.org

Electrophysiological evidence of adult human skeletal muscle fibres with multiple endplates and polyneuronal innervation

Zoia C. Lateva, Kevin C. McGill and M. Elise Johanson

Rehabilitation Research and Development Center, Veterans Affairs Palo Alto Health Care System, Palo Alto, CA 94304, USA

Electromyographic (EMG) signals were recorded using intramuscular electrodes at six different sites in the brachioradialis muscles during voluntary isometric contractions in four subjects. The potential waveforms and discharge patterns of up to 12 simultaneously active motor units were identified from each signal using computer-aided decomposition. Out of a total of 301 motor unit potentials identified, 23 potentials exhibited behaviour consistent with having been generated by muscle fibres that were innervated by two different motoneurons at widely separated endplates. These potentials discharged in association with two different motor units, but were blocked or delayed whenever the two motor units discharged within a few milliseconds of one another. The blocking was consistent with a collision or refractoriness when one motoneuron tried to excite the fibre while it was already conducting an action potential initiated by the other motoneuron. The delays were consistent with decreased conduction velocity associated with incomplete recovery of the fibre after a preceding action potential. From the temporal separation between the discharges of the two motoneurons that resulted in blocking, the spatial separation between the endplates was estimated to be between 26 and 44 mm. These findings challenge the classical concept of the motor unit as an anatomically distinct and functionally independent entity. It is suggested that the human brachioradialis muscle may contain both long, polyneuronally innervated fibres and short, serially linked, singly innervated fibres.

(Received 25 April 2002; accepted after revision 19 July 2002; first published online 16 August 2002)
Corresponding author: Z. C. Lateva: Rehabilitation Research and Development Center/153, Veterans Affairs Palo Alto Health Care System,3801 Miranda Avenue,Palo Alto, CA 94304,USA. Email: leteva@rrdmail.stanford.edu

It has been a dogma of classical anatomy and physiology that every normal adult mammalian skeletal muscle fibre is innervated by a single motoneuron. Indeed, it is now widely accepted that individual endplates in adult mammalian muscles are mononeuronally innervated. Neural development during late embryonic and early postnatal life in vertebrates includes stages in which intermingled branches of more than one axon overlie the acetylcholine receptors at the junctional site of the individual target myotube (Navarrete & Vrbova, 1993; Sanes & Lichman, 1999). However, in the first weeks after birth this transient focal polyneuronal innervation is transformed to mononeuronal innervation through the process of synaptic elimination. Similar processes occur during repair after nerve injury, when neuromuscular junctions are first reinnervated polyneuronally and then the supernumerary synapses are eliminated (Costanzo *et al.* 2000). The factors that govern the editing of synaptic connections are still not fully understood (Personius & Balice-Gordon, 2001; Keller-Peck *et al.* 2001), but the editing process is commonly believed to result in mononeuronal innervation of individual endplates (Navarrete & Vrbova, 1993; Vrbova *et al.* 1995).

There is growing evidence, however, that some mammalian muscles contain fibres with more than one endplate. These muscles include rat gracilis (Jarcho *et al.* 1952), rat latissimus dorsi (Zenker *et al.* 1990), guinea-pig sternomastoid (Duxson & Sheard, 1995), horse sternocephalic (Zenker *et al.* 1990), and human facial (Happak *et al.* 1997) and laryngeal (Rossi, 1990; Perie *et al.* 1997) muscles. The first four of these muscles are long, parallel-fibred muscles, in which multiple endplates are found along the entire length of the fibre, separated by distances ranging from 1 mm in embryonic muscle to 30 mm in adult muscle. The multiple endplates in the human facial and laryngeal muscles are found closer together, typically less than 150 μm apart. Twitch muscle fibres with multiple endplates are also known to exist in some frog skeletal muscles (Sandmann, 1885; Katz & Kuffler, 1941).

The existence of muscle fibres with multiple endplates raises the important question of whether these endplates are supplied by the same motoneuron or by different motoneurons. This question was first put forward over a century ago by Sandmann (1885) with respect to frog muscle, and it remains largely unanswered. Both possibilities

have intriguing physiological implications. If the endplates are innervated by the same motoneuron, that would imply the existence of processes during development that enable motoneurons to identify and establish connections to the same muscle fibres at widely separated locations. On the other hand, if they are innervated by different motoneurons, that would mean that muscle fibres can be shared between more than one motor unit. This would challenge the classical concept that the motor unit – 'an individual nerve fibre with the bunch of muscle fibres it activates' (Sherrington, 1930) – is an anatomically distinct and functionally independent entity.

Determining the innervation of multiple endplates on the same muscle fibre has proved to be technically difficult. Conventional histological methods are unable to follow individual nerve and muscle fibres over the necessary distances. Cholinesterase (ChE) staining, which is an effective method for investigating the distribution of endplates in whole muscle (Desmedt, 1958; Christensen, 1959; Coërs & Woolf, 1959; Aquilonius *et al.* 1984; Snobl *et al.* 1998), has also been applied in combination with microscopy to investigate endplate distributions on individual muscle fibres. ChE staining has been used with electron microscopic serial cross-sectioning to identify multiple endplates in embryonic muscle (Duxson & Sheard, 1995). It has also been used in combination with microdissection to investigate endplate distributions on some single adult muscle fibres in animals (Jarcho *et al.* 1952; Zenker *et al.* 1990) and humans (Happak *et al.* 1997). Perie *et al.* (1997) used double staining (for ChE activity and axons) and serial cross-sectioning to determine that the nearby multiple endplates (separated by less than 700 μm) in human laryngeal muscle fibres are innervated by the same motoneuron. However, these histological techniques have so far been inadequate for identifying the sources of innervation of the more widely separated multiple endplates in long, parallel-fibred muscles.

The innervation of multiple endplates has also been investigated by measuring the summation of twitches elicited by electrical stimulation of individual ventral root filaments (Hunt & Kuffler, 1954; Brown & Matthews, 1960; Sheard *et al.* 1999). The expectation is that if two filaments innervate some of the same muscle fibres, then the twitch produced when they are stimulated together will be less than the sum of the twitches produced when they are stimulated individually. However, this reasoning underestimates the complexity of the mechanical interactions between muscle fibres. Twitches of synchronously activated motor units generally do not sum linearly (Merton, 1954), and the summation is affected by the muscle composition (Troiani *et al.* 1999) and architecture (Trotter *et al.* 1995). For this reason, the results of these biomechanical studies have been contradictory, difficult to interpret and inconclusive.

Another approach for investigating the innervation of multiple endplates has been to measure the electrical response to stimulation. Katz & Kuffler (1941) studied the innervation of frog sartorius muscle by recording action potentials elicited by electrical stimulation of cut nerve branches. They found that action potentials elicited simultaneously at distinct endplate zones collided rather than passing one another, and therefore concluded that most of the fibres in the muscle were multiply innervated. McComas *et al.* (1984) also demonstrated collisions between action potentials evoked by surface stimulation at different sites over the human brachial biceps muscle. They interpreted these results as evidence for the existence of fibres with multiple endplates. In both these studies, the stimulation involved whole nerve branches rather than individual motoneuron axons, so it was not possible to tell whether individual muscle fibres were innervated by the same or by different motoneurons.

In this paper, we have studied the innervation of multiple endplates in a normal adult human muscle using a different electrophysiological approach. The muscle studied is the brachioradialis muscle, a long, parallel-fibred muscle of the arm. The approach involves analysing motor unit potential (MUP) waveforms and discharge patterns obtained by decomposition of electromyographic (EMG) signals recorded during voluntary contractions. If a fibre is innervated by two motoneurons, then it can be expected to discharge in association with both of them and to contribute similarly shaped components to both MUPs. However, when both motoneurons discharge close together in time, one of the components should be blocked because of a collision in the muscle fibre. We indeed were able to detect components in the signals that exhibited this behaviour. Moreover, by analysing the temporal separation between the discharges that resulted in collisions, we were able to estimate the spatial separation between the two endplates. Our results thus provide evidence that some muscle fibres in brachioradialis receive polyneuronal innervation at widely separated endplates.

METHODS

Four volunteers (3 males; 1 female) aged between 25 and 49 years participated in five experimental sessions (one subject participated in two sessions on two different days). None of the subjects had any history of neuromuscular disease. The experimental procedures were approved by the Stanford University Committee on the Use of Human Subjects in Research and conformed to the Declaration of Helsinki. Informed written consent was obtained from all the subjects.

Experimental setting

Subjects were seated comfortably with their right forearm supported in elbow flexion and neutral forearm rotation. EMG signals were recorded simultaneously from multiple sites in the brachioradialis muscle. The brachioradialis muscle was identified during resisted elbow flexion. Two or three fine wire electrodes were inserted 30–40 mm apart along the muscle axis between the

elbow crease and the distal end of the palpable muscle belly. The electrodes consisted of sterile, 50 μm, stainless steel, insulated fine wires with 1–2 mm exposed recording surface at the tips. They were inserted using a 25 gauge, 37 mm needle that was then withdrawn. The subjects were instructed to activate the brachioradialis and adjacent forearm muscles to confirm correct electrode placements. The fine-wire electrodes remained in place during the entire experiment. EMG activity was also recorded using a monopolar needle electrode (27 gauge, 25 mm, 1 mm exposed recording surface). It was inserted at different points along the muscle belly and manipulated by the examiner during the experiment in order to sample different parts of the muscle. A reference electrode was placed on the surface of the arm over the distal brachioradialis tendon and a ground electrode was placed on the medial surface of the forearm.

EMG recordings

EMG signals were collected during moderate (20 s long) voluntary isometric contractions. The subject flexed the elbow against manual resistance provided by the examiner. The level of contraction was determined by having the subject adjust the level until the examiner judged that the signal from the needle electrode contained activity from several motor units. The subject was provided with auditory feedback in order to maintain the level of contraction as constant as possible. After each contraction, the subject relaxed, and the needle electrode was repositioned to another location. Sometimes recordings were made at more than one different level of contraction before moving the needle electrode. The signals were recorded monopolarly between the fine wire or needle electrode and the reference electrode. The signals were amplified (Nicolet Viking, Madison, WI, USA; filter settings, 2–5 kHz), sampled at 10 kHz and stored on computer.

EMG analysis

The recorded signals were analysed to identify the individual motor unit potentials (MUPs) using computer-aided decomposition. We have developed an interactive computer program that allows a skilled operator to identify and sort out every discharge in a moderately complex EMG signal. The program also makes it possible to 'subtract out' the activity of MUPs that are not of interest in order to reveal the activity of other MUPs more clearly.

The decomposition procedure can be understood by reference to Fig. 1, which depicts the computer screen during the analysis. The signal is first digitally high-pass filtered at 1 kHz. Since the amplitude of the high frequency components of extracellular muscle fibre action potentials decreases rapidly with distance, this filtering step accentuates the MUPs of motor units with at least one fibre close to the recording electrode and attenuates the MUPs of more distant motor units and the background noise. The high pass-filtered signal is displayed in 100 or 200 ms long segments (Fig. 1*A*), along with the templates of the active MUPs (Fig. 1*C*). The templates can be determined automatically by the program or manually by selecting one of the spikes in the signal. The spikes are identified by matching them against the templates. The matching can also be done automatically, or it can be done manually by selecting one of the templates. The program automatically aligns the selected template to give the best fit to the signal. The alignment is performed using interpolation to avoid time-quantization errors

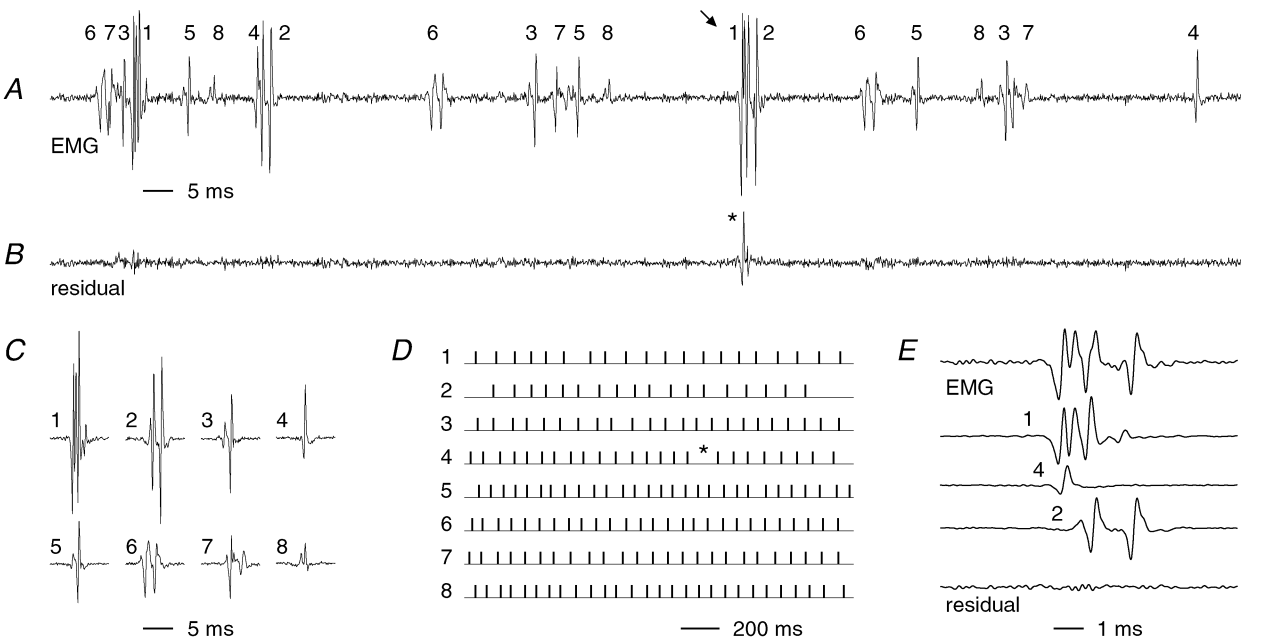

Figure 1. Computer displays utilized by the human operator during the decomposition of an EMG signal

A, a segment of the EMG signal to be analysed. The signal has been high-pass filtered at 1 kHz. The numbers show the identities of the MUPs that have already been identified. *B*, the residual signal obtained by subtracting the templates of the identified MUPs from the actual signal. *C* and *D*, the templates and discharge patterns of the identified MUPs. In the example shown here, the decomposition is complete except for one superimposition (*A*, arrow) that has not been fully resolved, as indicated by the spike in the residual signal (*B*, *) and the gap in the discharge patterns (*D*, *). *E*, a close-up of the superimposition with MUP 4 included as well as MUPs 1 and 2. After automatic alignment, these three MUPs give a good fit to the actual signal, as shown by the small residual.

(McGill & Dorfman, 1984), and using a sophisticated algorithm to resolve superpositions of multiple templates (Fig. 1*E*; McGill, 2002). The residual difference is displayed to show the goodness of fit (Fig. 1*B*). The identified motor unit discharge patterns are also displayed (Fig. 1*D*).

The operator verifies the accuracy of the decomposition by examining the residual signal and the discharge patterns. Mistakes can be recognized by the presence of excessive noise in the residual signal and by the presence of gaps, extra discharges or uneven intervals in the discharge patterns. For example, in the decomposition shown in Fig. 1, the gap in the discharge pattern of MUP 4 (Fig. 1*D*, *) and the spike in the residual signal indicate that the signal was not completely decomposed. Inspection shows that the superposition indicated by the arrow was not fully resolved. Dragging the template of MUP 4 to the location of the spike fills in the discharge pattern and results in a good fit to the superposition, as shown in the close-up display (Fig. 1*E*). In this example, the complete, regular discharge patterns and the small amplitude of the residual signal give high confidence that the decomposition is accurate.

The signals recorded from different electrodes during the same contraction were decomposed individually. MUPs from different electrode sites were judged to belong to the same motor unit if their discharge patterns were identical except for a fixed offset that could be attributed to propagation delay.

RESULTS

We analysed signals from 34 different contractions, identifying from four to 12 MUPs per signal. While decomposing the signals, we noticed that a number of MUPs had gaps in their discharge patterns or excessive jitter in their waveforms. These MUPs always occurred in pairs, with the MUPs in each pair often having similar shapes. We have never observed irregularities like this in other muscles we have studied, such as first dorsal interosseous, brachial biceps, tibialis anterior and gastrocnemius. However, these irregularities occurred in 16 of the signals from brachioradialis, including at least one signal from each subject. We therefore examined these signals more closely to try to find an explanation for the irregularities. Sets of MUPs from three different signals that exhibited irregularities are presented here as examples.

First example

The pair of MUPs, labelled mup1 and mup2, in Fig. 2 exhibited the typical pattern of discharge and waveform irregularities. They were recorded by the needle electrode at a site 90 mm distal to the elbow crease in subject 3. This example is instructive for two reasons. First, this was one of the sites at which recordings were made during two different contractions. The irregularities only occurred during the stronger contraction, when both of the MUPs were active. This confirmed that the irregularities involved an interaction between the two motor units. Second, the discharges of one of the motor units were also detected simultaneously by one of the fine wire electrodes. This provided an insight into the nature of the irregularities.

The discharge pattern of mup1 during the first contraction is shown in trace 1 of Fig. 2*A*. Mup1 was one of three MUPs recorded in the needle-electrode signal. It discharged regularly with a mean inter-discharge interval of 104 ± 18 ms. Trace 2 of Fig. 2*A* shows the discharge pattern of mup1*, a MUP recorded by a fine-wire electrode located 60 mm distal to the elbow crease. Its discharges were always time-locked to those of mup1, indicating that they both were produced by the same motor unit. The waveforms of mup1 and mup1* are shown in traces 1 and 2 of Fig. 2*B*. Mup1 had a simple shape with minimal discharge-to-discharge variability. It was offset from mup1* by 4.9 ms, which can be attributed to conduction delay between the two recording sites. Thus during the first contraction, mup1 did not exhibit any irregularities.

The discharge patterns and waveforms during the second contraction are shown in the bottom three traces of Fig. 2*A* and *B*. This contraction was somewhat stronger than the first, with a total of eight MUPs being detected in the needle-electrode signal. Both mup1 and mup2 were active during this contraction, and they both exhibited irregularities. The most prominent irregularity was that mup1 had frequent gaps in its discharge pattern (Fig. 2*A*, trace 3, ×). Its discharges remained time-locked to those of mup1*, but mup1* discharged regularly throughout the entire contraction (Fig. 2*A*, trace 4; mean inter-discharge interval 86 ± 15 ms), even during the gaps when mup1 was not detected. This showed that the gaps in the discharge pattern of mup1 were not due to de-recruitment of the motoneuron, but rather to a failure of transmission in some of the muscle fibres. Mup2 had a complex shape consisting of two main components that exhibited a large amount of jitter (Fig. 2*B*, trace 5). The second component (mup2b) occasionally failed to occur (Fig. 2*A*, trace 5, ×), although the first component (mup2a) discharged continuously throughout the entire contraction. Moreover, component mup2b was very similar in shape to mup1.

Further analysis of the signals revealed that every missing occurrence of mup1 was immediately preceded by a discharge of mup2. This can be seen more clearly in traces 1–7 of Fig. 2*C*, which show several instances in which mup2 and mup1* discharged close together in time. As long as mup2 discharged at least 23 ms before the expected occurrence time of mup1 (filled arrows), mup1 always occurred (traces 1–3, open circles). But whenever mup2 discharged less than 21.5 ms before this time, mup1 always failed to occur (traces 4–7, ×).

Conversely, the jitter in the waveform of mup2 was associated with the activity of mup1. This can be seen in traces 8–14 of Fig. 2*C*, which show instances in which mup1 discharged shortly before mup2. As long as mup1 discharged at least 15 ms before mup2, the waveform of mup2 was relatively stable, as shown by the superimposed

signals in trace 8. But whenever mup1 discharged less than 15 ms before mup2, component mup2b was delayed and attenuated (traces 8–12, filled circles). The closer together the two MUPs discharged, the more pronounced was the effect. When they discharged very close together (mup1 discharging less than 3.5 ms before the normal occurrence time of mup2b, filled arrows), mup2b failed to occur altogether (traces 13–14).

Although the two components of mup2 usually occurred in superposition, it was possible to determine their individual waveforms. The waveform of the first component (mup2a) was obtained from Fig. 2*C* (trace 12), in which the two components were widely separated and did not overlap. The waveform of the second component (mup2b) was then obtained by subtracting mup2a from the normal mup2 waveform (Fig. 2*C*, trace 8). The waveforms of the two components are shown in Fig. 3*B*. It can be seen that component mup2b is virtually identical to mup1. Moreover, they both have a simple shape that could have been generated by a single muscle fibre.

Explanation of irregularities. Careful consideration of these observations led us to what we believe is the only plausible explanation for the discharge and waveform irregularities; that components mup1 and mup2b were

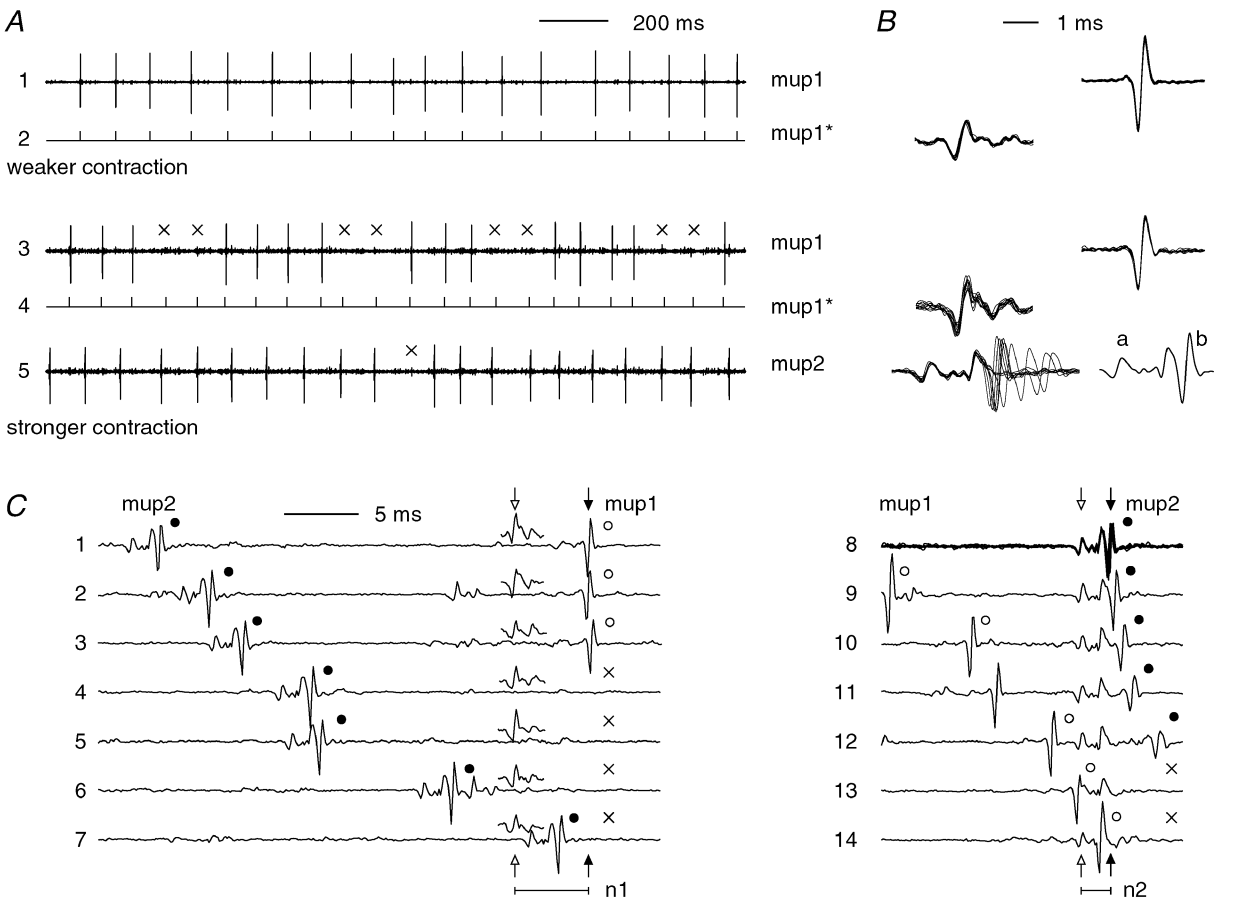

Figure 2. Typical MUP pair that exhibited waveform and discharge irregularities

A, discharge patterns of two motor units during a weaker contraction (traces 1 and 2) and during a stronger contraction (traces 3–5). The first motor unit was recorded simultaneously by the needle electrode (mup1) and by a fine-wire electrode (mup1*). The second motor unit was recorded only by the needle electrode (mup2). × indicates gaps in the discharge pattern of mup1 (trace 3) and a missing occurrence of the second component of mup2 (trace 5). Traces 1, 3 and 5 show actual signals from which the activity of the other identified MUPs has been subtracted, to show that the missing occurrences were not due to decomposition errors. *B*, the waveforms of the MUPs in *A*. Several occurrences of each MUP are superimposed to show the discharge-to-discharge variability or 'jitter'. A single occurrence of mup2 is shown on the right-hand side in the lower trace to show its two components, mup2a and mup2b. *C*, several segments of EMG in which mup1 and mup2 discharged close together in time. The signals are sorted in order of the interval between the two MUPs. The occurrences of mup1 and mup2b are marked ○ and ●, respectively. In traces 1–7 the signals are aligned by the discharges of mup1* (insets, open arrows). In traces 8–14 they are aligned by the stable component of mup2 (mup2a, open arrows). The usual discharge times of mup1 and mup2b (with respect to the occurrence times of mup1* and mup2a) are indicated by the filled arrows, and n1 and n2 indicate the normal inter-component intervals. × indicates the missing occurrences of mup1 and mup2b.

produced by the same single muscle fibre, which was innervated by two different motoneurons at two widely separated endplates. This situation is illustrated schematically in Fig. 3*A*. Line f1 represents the doubly innervated fibre, which was in essence shared between both motor units. Line f2 represents the set of fibres responsible for component mup2a, which were innervated only by the second motoneuron. Both motoneurons presumably innervated other muscle fibres as well, but f1 and f2 depict those fibres that produced detectable potentials at the electrode site.

The similarity between the shapes of mup1 and mup2b is explained by the fact that they were both produced by the same muscle fibre (Fig. 3*B*). Whenever motoneuron mn1 discharged by itself, it generated an action potential in fibre f1, which was recorded by the electrode as mup1. Whenever mn2 discharged by itself, it generated action potentials in both f2 and f1, and the sum of these potentials was recorded as the two overlapping components of mup2.

The blocking and jitter came about when both motoneurons tried to activate the shared fibre at the same time. Whenever this happened, the action potentials from the two endplates either collided, or one of them failed to be initiated because the muscle fibre was refractory, or one of them was delayed because the muscle fibre had incompletely recovered. The details of these interactions will be considered in greater detail in Discussion.

Second example

A second pair of MUPs that exhibited discharge and waveform irregularity is shown in Fig. 4. They were two of eight active MUPs recorded by the needle electrode at a site 80 mm distal to the elbow crease in subject 1. This pair was similar to the pair in the first example in that one of the MUPs (mup1) had gaps in its discharge pattern (Fig. 4*A*), while the other (mup2) exhibited a large jitter (Fig. 4*B*). They differed in that the volatile component of mup2 did not have exactly the same shape as mup1 (Fig. 4*B*). Moreover, during this contraction neither motor unit was detected at another recording site.

Since no independent record of the discharges of the first motor unit was available, it was not possible to verify directly that the gaps in the discharge pattern of mup1 were due to blocked transmission and not to de-recruitment. However, the histogram of its inter-discharge intervals (Fig. 4*C*) showed that most of the intervals fell within the range of 35 to 75 ms (mean 59 ms), and that the longer intervals, which corresponded to the gaps, were integer multiples of this. This is the type of histogram that would be expected if discharges were missing from an otherwise regular train, and it strongly suggests that the gaps were due to blocked transmission.

As in the first example, the behaviour of the volatile component of mup2 was associated with the activity of mup1, as shown in Fig. 4*D*. Whenever mup1 discharged immediately before mup2, the first component of mup2 was delayed or failed to occur. The gaps in the discharge pattern of mup1 were also associated with the activity of mup2. This can be seen in Fig. 4*E*, which depicts several consecutive inter-discharge intervals of mup2. The mean inter-discharge interval of mup2 was 74 ms (i.e. longer than that of mup1). The expected times of the missing occurrences of mup1 were estimated to be at the midpoints (or third-way points) of the gaps in the discharge pattern of mup1 and are shown by ×. Mup1 always failed to occur whenever its expected discharge time fell within a 21 ms interval after a discharge of mup2 (traces 2 and 6).

Since components mup1 and mup2a in this example behaved in the same way as in the first example, we concluded that they must also have been produced by one or more doubly innervated muscle fibres. However, in this case, the waveforms of the two components did not have simple shapes, and their shapes were not exactly the same.

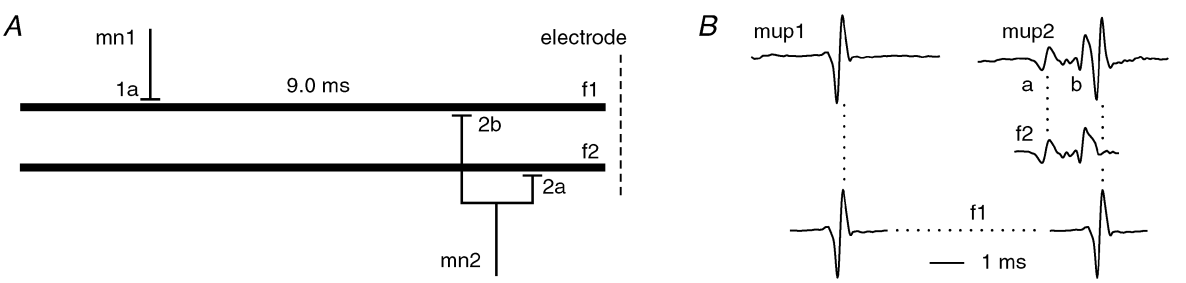

Figure 3. Innervation diagram for the MUPs in Fig. 2

A, f1 and f2 are two muscle fibres or groups of muscle fibres innervated by the two motoneurons mn1 and mn2. Fibre f1 is innervated by both motoneurons. The electrode was located to one side of both endplates, but closer to the endplates of mn2. The time needed for a wave of depolarization to propagate between endplates 1a and 2b was calculated to be 9 ms, as described in Discussion. *B*, composition of the MUP waveforms; mup1 consists of a single component arising from the shared fibre f1; mup2 is the sum of two components, mup2a which arises from f2, and mup2b, which arises from the shared fibre f1.

This can be explained by considering the interesting event that took place in trace 5 of Fig. 4*E*. In that trace, mup1 was due to discharge just at the end of the interval in which it would normally have been blocked by mup2. A discharge did occur, but it was small and resembled only the initial part of the waveform of mup1. This happened twice again during the 20 s signal, leading us to suspect that mup1 actually consisted of two subcomponents, one equal to the small waveform in trace 5, and the other equal to the remainder. Indeed, it proved possible to reconstruct component mup2a exactly, by adding these two subcomponents together at a slightly different offset. Both of

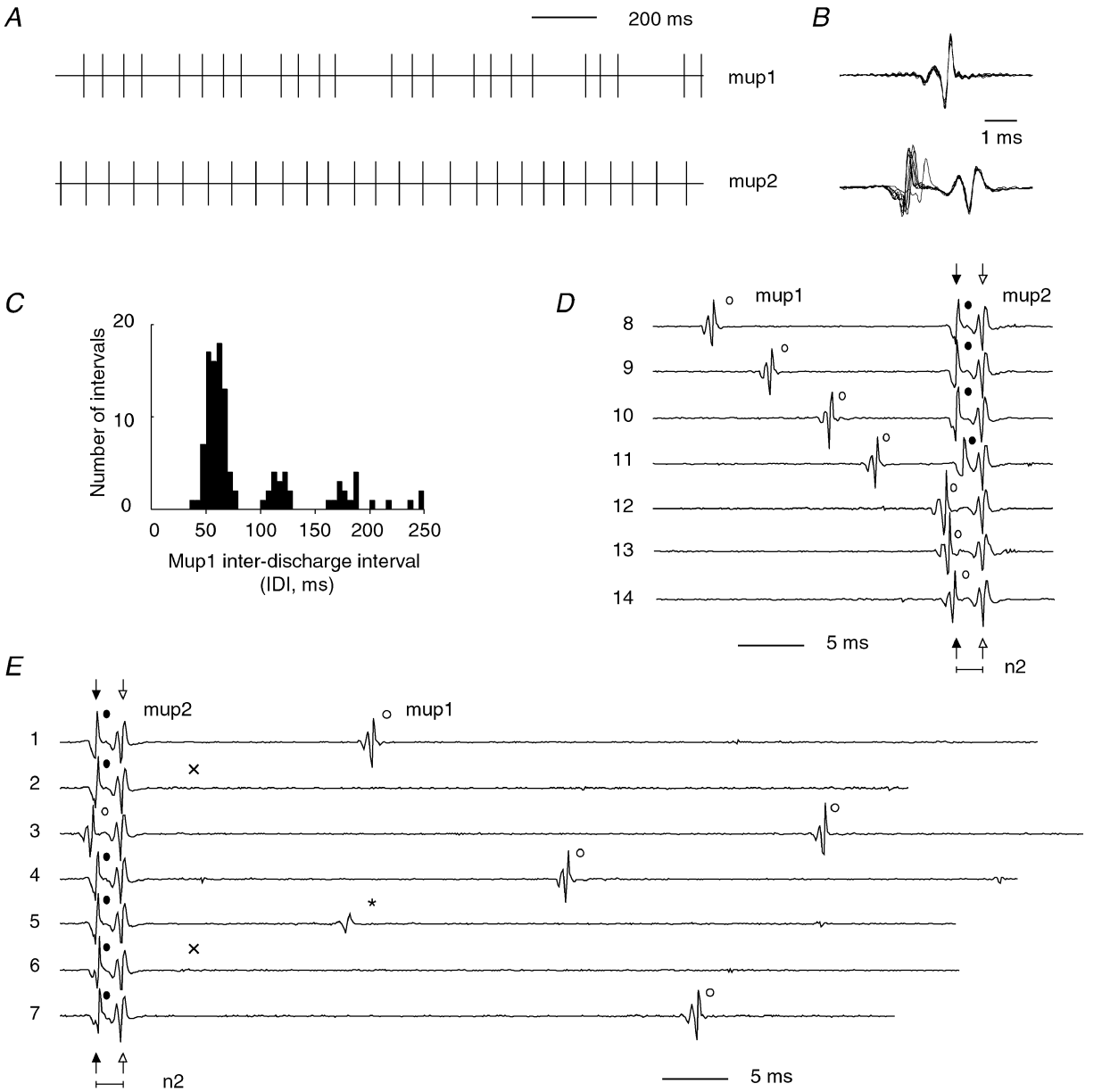

Figure 4. Second example of a MUP pair that exhibited irregularities

A, discharge patterns of the two MUPs. *B*, waveforms of the two MUPs. *C*, histogram of inter-discharge intervals for mup1. *D*, several segments of EMG signal in which mup1 discharged shortly before mup2. They are sorted by inter-unit interval, and aligned by the stable component of mup2 (open arrows). The occurrences of mup1 and the volatile component of mup2 are indicated by ○ and ●, respectively. The normal occurrence time of the volatile component of mup2 is indicated by the filled arrows, the missing occurrences by ×, and the normal inter-component interval by n2. *E*, several consecutive segments of EMG signal, aligned on the consecutive discharges of the stable component of mup2 (open arrows). The lengths of the traces correspond to the consecutive inter-discharge intervals of mup2. The activity of all the other MUPs except mup1 and mup2 has been subtracted out. The estimated times of the missing occurrences of mup1 are indicated by ×. The occurrence of mup1 in trace 5 (*) includes only one subcomponent.

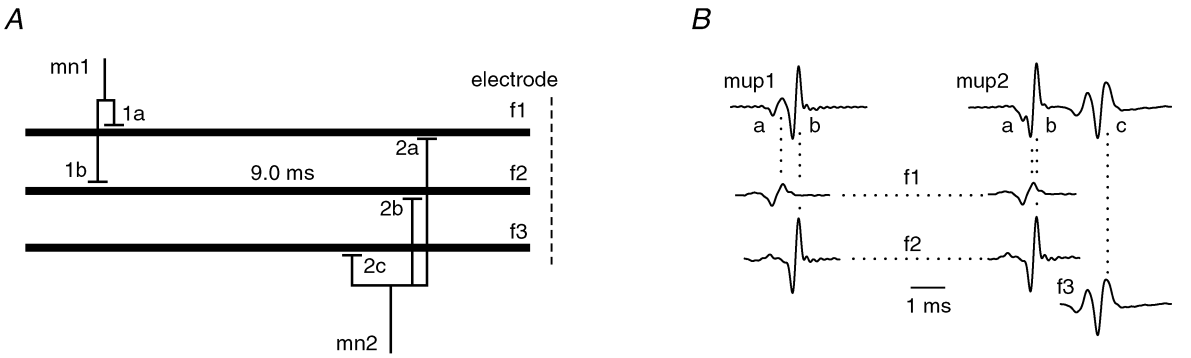

Figure 5. Innervation diagram for the MUPs in Fig. 4

A, f1 and f2 are shared muscle fibres, innervated by both motoneurons. The endplates are slightly further apart on f1 than on f2. The fibre f3 is only innervated by motoneuron mn2. The estimated propagation time between endplates 1b and 2b is 9 ms. *B*, composition of the MUP waveforms. The potentials from f1 and f2 sum together in slightly different temporal configurations in the two MUPs due to the difference in the distance between their endplates.

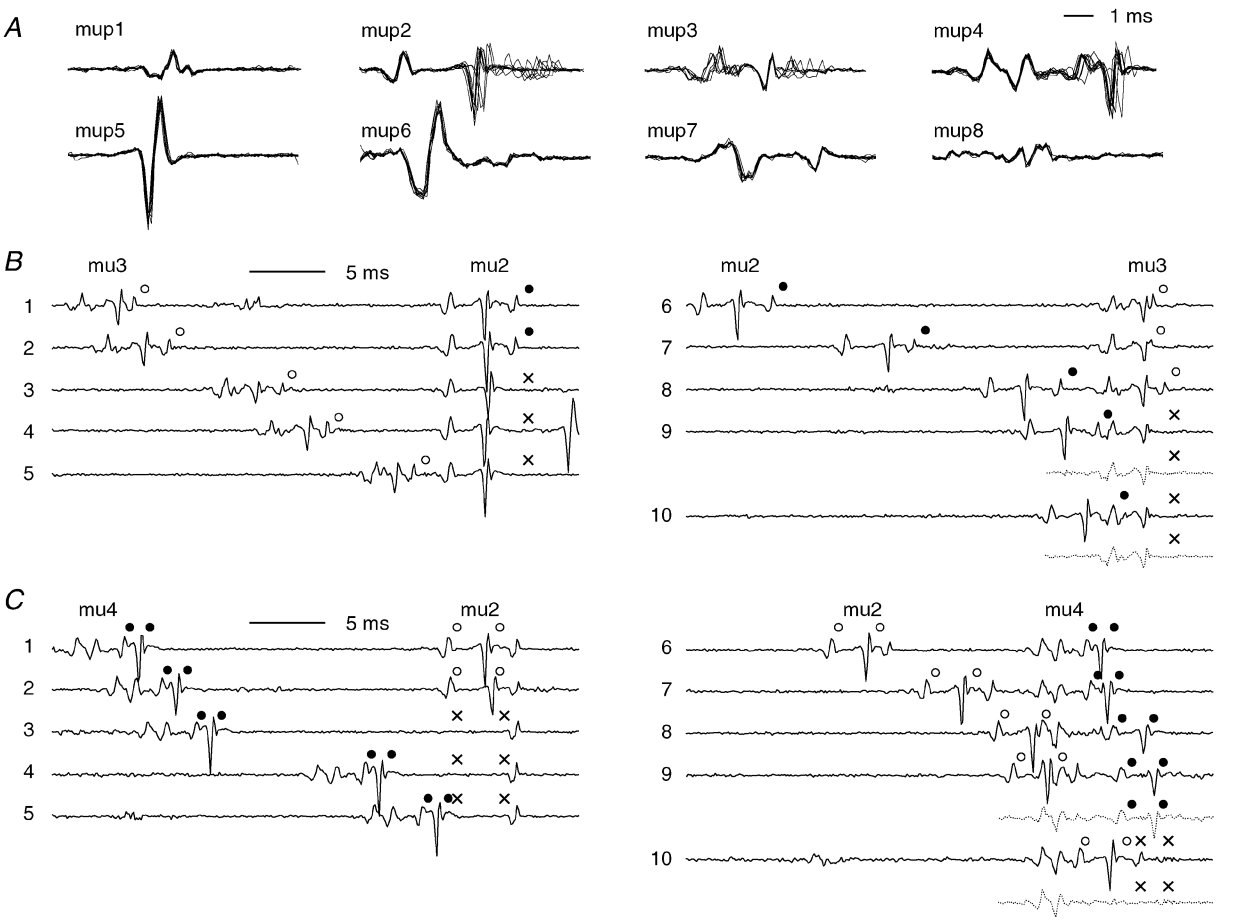

Figure 6. Third example of irregularities

A, waveforms of eight MUPs detected by the needle electrode. Mups 1–4 have components with similar shapes and excessive jitter. *B* and *C*, segments of the EMG signal in which pairs of MUPs with similarly shaped components discharged close together in time. In each panel, the components associated with the different MUPs are marked by ○ and ●. × indicates the missing occurrences. Some of the traces have been replotted (dotted lines) with the MUP that caused the blocking subtracted out to show the results of the blocking more clearly.

Table 1. Summary of motor unit data by subject and electrode location

	Electrode location (mm distal to elbow crease)						
Subject	0–20	21–40	41–60	61–80	81–100	101–120	Total
1. (49 m)	0/8	0/11	0/9	1/8	3/17	4/8	8/61
1. (49 m)	0/7	1/31	0/8	3/25	1/15	—	5/86
2. (26 m)	0/11	—	0/7	0/9	1/13	0/8	1/48
3. (28 m)	—	1/20	1/18	—	2/20	1/8	5/66
4. (31 f)	0/12	3/14	1/6	0/8	—	—	4/40
Total	0/38	5/76	2/48	4/50	7/65	5/24	23/301

The first value in each entry is the number of doubly innervated fibres identified. The second value is the total number of motor units identified. Each entry corresponds to one or more recordings at different electrode locations within the indicated range. When more than one contraction was recorded at the same location, only the results from the most forceful contraction are shown. A dash indicates no recordings were made. Subject 1 was tested twice on separate occasions. The age and gender of each subject are indicated.

the subcomponents had simple waveforms that could have been generated by single muscle fibres.

The irregularities in these MUPs are thus explained by the innervation diagram in Fig. 5*A*. The two motor units shared two fibres (f1 and f2), with the endplates on f2 being slightly further apart than those on f1. Whenever either motoneuron discharged by itself, it initiated action potentials in both fibres. Depending on which motoneuron discharged, the potentials summed together in a slightly different temporal relationship to produce mup1 or mup2a (Fig. 5*B*). Whenever the two motoneurons discharged at about the same time, the action potentials from one of the motoneurons were blocked by collision or refractoriness, resulting in a missed occurrence of one of the components. Occasionally, a nerve impulse from mn1 arrived at just the right time after the passage of an action potential from mn2 to find f1 sufficiently recovered to be excitable while f2 was still refractory. This resulted in the blocking of the action potential in f2 but not in f1, as happened in trace 5 of Fig. 4*E*.

Third example

The most complex example of MUP irregularity that we observed is shown in Fig. 6. This was a signal recorded by the needle electrode at a site 116 mm distal to the elbow crease in subject 1. There were eight active MUPs (Fig. 6*A*), four of which (1–4) had components that resembled one

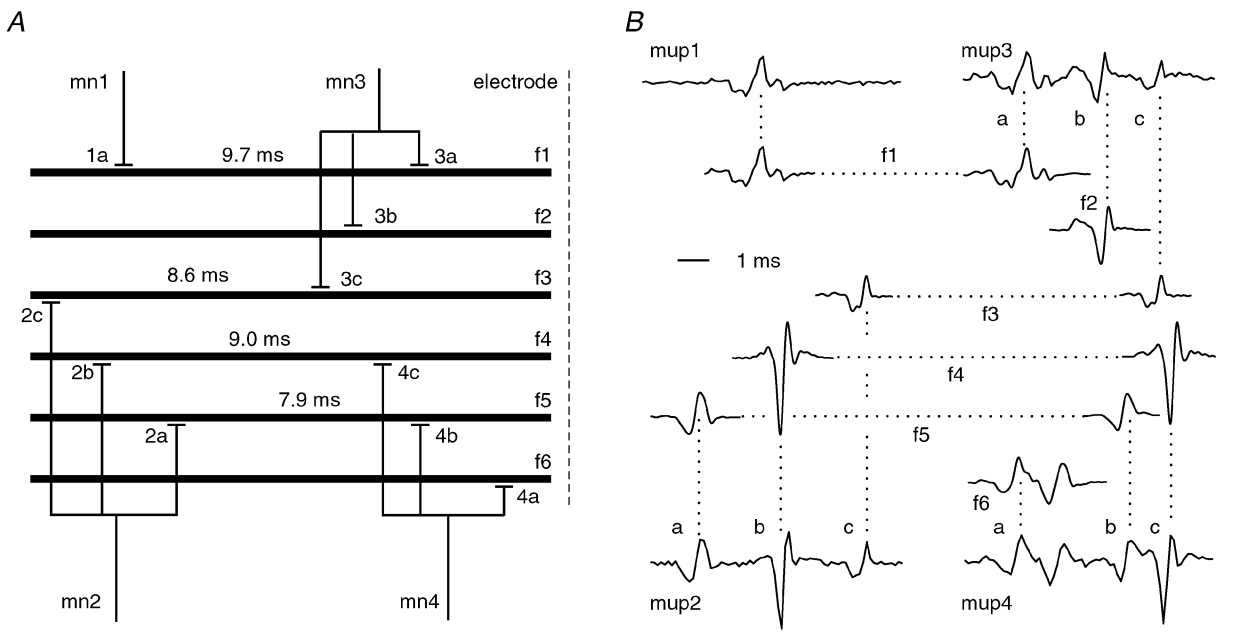

Figure 7. Innervation diagram for the MUPs in Fig. 6

A, mups 1–4 were generated by six fibres or groups of fibres, four of which were doubly innervated. The estimated propagation times between the endplates of the shared fibres are as shown. *B*, composition of the MUP waveforms. Each of the components of mups 1–4 came from one of the muscle fibre groups, as shown.

another and exhibited excessive jitter and intermittent blocking (Fig. 6*B* and *C*). The other four (Fig. 6*A*, mup5–mup8) did not exhibit excessive jitter or blocking, even though some of them had multiple components.

An analysis of the waveform components and the blocking patterns showed that mup1–mup4 were made up of six separate components that were generated by six separate muscle fibres or sets of muscle fibres according to the innervation diagram in Fig. 7*A*. The way in which the potentials from the six sets of fibres sum together to give the four MUPs is shown in Fig. 7*B*. Two of the sets of fibres were singly innervated while four were doubly innervated. For example, set f1 was innervated both by mn1 and mn3, and was responsible for mup1 and component mup3a. Notably, two of the sets of fibres, f4 and f5, were both innervated by the same pair of motoneurons.

Distribution of doubly innervated fibres

Overall, we observed evidence of 23 doubly innervated fibres or sets of fibres. These are summarized by subject and by electrode position in Table 1. Doubly innervated fibres were detected in every subject, although only one instance was detected in subject 2, whereas at least four instances were detected in each of the other subjects. Subject 1 was examined twice, and doubly innervated fibres were detected on both occasions. There was no clear relationship between electrode position and the frequency of detection. The MUP components from the shared and non-shared fibres were not always as distinct as in the preceding examples. Sometimes the component from the shared fibre was small, or completely superimposed on the other component, making the incidence of blocking more difficult to detect.

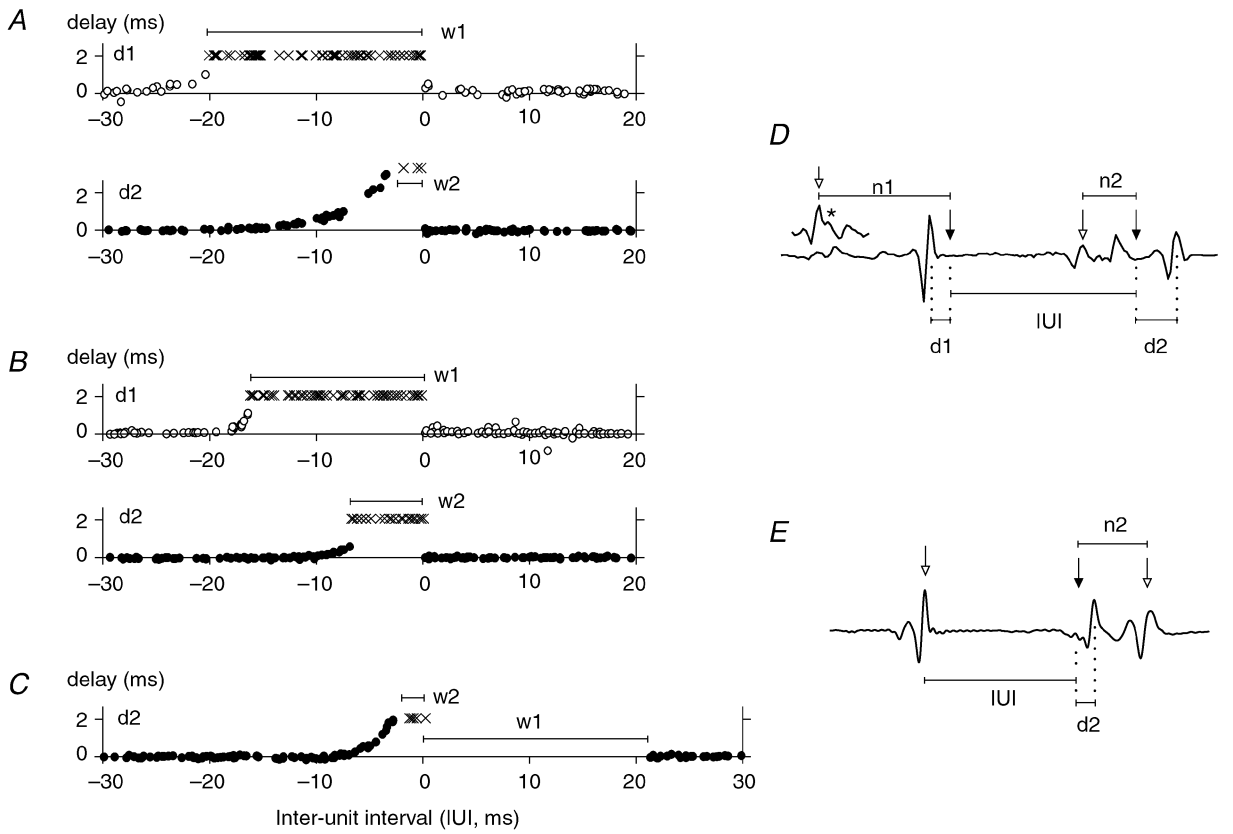

Figure 8. The delay and blocking of the MUP components

A–C, delays of the volatile components as a function of the inter-unit interval for three pairs of MUPs that exhibited irregular behaviour. *A*, MUPs from Fig. 2, *B*, MUPs not shown elsewhere, and *C*, MUPs from Fig. 4. × indicates the blocked occurrences, and w1 and w2 indicate the 'blocking windows'. The variables were measured as shown in *D* and *E*. *D*, stable components were detected for both MUPs (as in *A* and *B*). The actual occurrence times of the stable components are shown by the open arrows. From these times and the normal inter-component intervals (n1, n2), the expected occurrence times of the volatile components were determined (filled arrows). The delays (d1, d2) were measured between the actual and expected occurrence times of the volatile components. The inter-unit interval (IUI) was measured between the expected occurrence times of the two volatile components. *E* a stable component was detected for only one of the MUPs (as in *C*). In this case the delay could be measured for only one of the volatile components (d2) and the IUI had to be estimated using the actual occurrence time of the other volatile component.

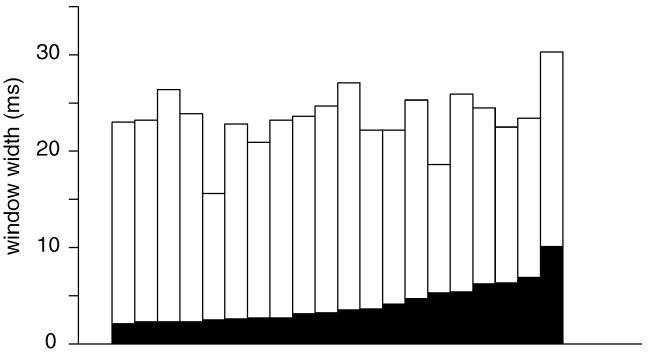

Figure 9. Widths of blocking windows for 20 pairs of MUP components from doubly innervated fibres

The width of the narrower window is shown by the filled bars, and the width of the wider window by the open bars. The bars have been sorted according to the width of the narrower window.

Quantitative assessment of blocking and jitter

The interactions between pairs of MUPs from three contractions are shown in a quantitative way in Fig. 8. Each plot shows the amount by which one of the volatile components (i.e. one of the components produced by a shared fibre) was delayed as a function of the temporal separation between the MUPs (inter-unit interval, IUI) for every discharge during an entire contraction. The instances in which the volatile component failed to occur are indicated (×). The plots in Fig. 8*A* and *C* correspond to the MUPs from examples 1 and 2. In Fig. 8*C*, the delay could only be determined for one of the volatile components, since no stable component associated with the other volatile component was detected. This is also the reason for the gap in the plot. The way in which the delays and separations were measured is explained in Fig. 8*D* and *E*.

These plots show the types of interactions that were described in conjunction with Fig. 2*C*. Immediately preceding the expected occurrence time of each volatile component was a time window, which we will refer to as the 'blocking window', during which a discharge of the other motor unit prevented the component from occurring. Preceding the blocking window was an interval during which a discharge of the other motor unit caused the component to be delayed. The delay increased exponentially with decreasing inter-unit interval (IUI), up until the IUI that resulted in blocking. In general, the components with shorter blocking windows exhibited larger maximum delays. In cases in which stable components were not available for both MUPs, such as shown in Fig. 8*C*, the width of the gap provided an estimate of the width of the second blocking window.

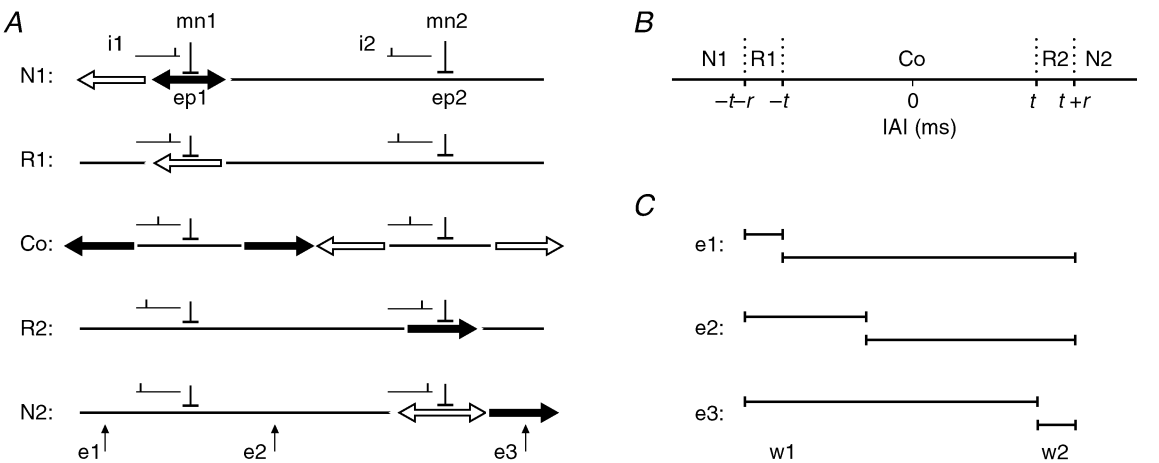

Figure 10. Blocking in a doubly innervated fibre

A, schematic representations of a muscle fibre f that is innervated by motoneurons mn1 and mn2 at endplates ep1 and ep2. Five different situations can occur, depending on the relative arrival times of the two nerve impulses (i1 and i2). N1, i1 arrives at ep1 after the wave of depolarization from ep2 (open arrow) has passed. Two new waves are initiated (filled arrows), that is, no blocking occurs. R1, i1 arrives during the passage of the wave from ep2. No new action potential is initiated due to the refractoriness of the muscle fibre. Co, i1 and i2 arrive close together in time. Two waves are initiated at each endplate, but the central ones collide and fail to propagate past the point of collision. Situations R2 and N2 are identical to R1 and N1 with the roles of the two endplates reversed. *B*, diagram showing the relationship between the difference in nerve impulse arrival times (inter-arrival interval, IAI) and the type of blocking. The time required for the wave of depolarization to propagate from one endplate to the other is indicated by *t*, the absolute refractory period by *r*. *C*, the blocking windows (w1 and w2, corresponding to mn1 and mn2) for the three electrode sites (e1, e2, e3) indicated in *A*.

It was possible to determine reliably the blocking window widths for 20 of the doubly innervated fibre sets. The widths are plotted in Fig. 9, with the filled and open bars corresponding to the narrower and wider windows, respectively. The narrower window always had a width of at least 2.1 ms, and it ranged up to 10.1 ms. In 12 fibres, the width of the narrower window clustered in the range from 2.1 to 3.6 ms. The combined width of the two windows had a fairly narrow range, with a mean value (± S.D.) of 23.5 (± 3.1) ms. For all but three of the fibres the combined width fell in the range from 21 to 27 ms.

DISCUSSION

The main finding of this study was that there are muscle fibres in the adult human brachioradialis muscle that receive innervation from two different motoneurons at widely separated endplates. Their existence was revealed by the irregular behaviour of their action potentials during voluntary contractions when both co-innervating motoneurons were active. Although the existence of these fibres has yet to be confirmed histologically, it is difficult to imagine any other explanation that could account for the observed electrophysiological evidence. The finding of doubly innervated muscle fibres raises many further questions about their distribution, architecture, development, physiological purpose and neural control.

Blocking in doubly innervated fibres

In a singly innervated muscle fibre, the arrival of a nerve impulse at the motor endplate initiates an action potential consisting of two waves of depolarization that propagate away from the endplate in opposite directions along the fibre. In a doubly innervated fibre, action potential transmission from one or both endplates can be blocked when both motoneurons try to activate the fibre at the same time. The blocking takes place by two different mechanisms, refractoriness or collision, depending on the relative arrival times of the two nerve impulses. The possible situations are illustrated schematically in Fig. 10*A*. Each trace depicts a different interval between the nerve impulse arrival times (i1 and i2).

The middle trace (Co) in Fig. 10*A* shows the case in which the two nerve impulses arrive close together in time. Each impulse initiates an action potential at its endplate. The two outer waves of depolarization propagate to the ends of the fibre in the normal manner, but the two inner waves collide at some point between the endplates and fail to propagate beyond the point of collision.

The second and fourth traces (R1 and R2) show the cases in which the nerve impulses arrive somewhat further apart in time, such that the later one arrives at its endplate during the passage of the wave of depolarization initiated by the earlier one. The muscle fibre membrane is refractory due to the wave of depolarization, and the nerve impulse fails to re-excite it. The wave of depolarization continues to propagate normally, but no action potential is initiated by the nerve impulse that arrives later.

The first and last traces (N1 and N2) show the cases in which the nerve impulses arrive even further apart in time, such that the later one arrives after the passage of the wave of depolarization initiated by the earlier one. The muscle fibre membrane is no longer absolutely refractory, and so the later arriving nerve impulse is able to re-excite it. There is no blocking in this case, but the second action potential may be slowed if the muscle fibre has not recovered fully. The slowing will be discussed in greater detail in the next section.

The way in which the blocking is related to the relative timing of the nerve impulses is shown in Fig. 10*B*. The ordinate shows the inter-arrival time interval (IAI) between the nerve impulses. The labels Co, R and N indicate the ranges that correspond to collision, blocking due to refractoriness and no blocking, respectively. The IAI that corresponds to the end of the collision region and the beginning of the refractory region is equal to the time needed for a wave of depolarization to propagate between the two endplates (t). The width of the refractory region equals the length of time that a section of the fibre remains refractory during the passage of a wave of depolarization. This time is known as the absolute refractory period (r).

Blocking windows. The blocking of propagation in a doubly innervated muscle fibre manifests itself as a missing occurrence of a MUP component in the EMG signal. Every instance of blocking, whether because of refractoriness or collision, blocks the occurrence of one MUP component. In the case of refractoriness, the component that is blocked is the one from the blocked endplate. In the case of a collision, the component that is blocked depends on the location of the electrode. If the electrode is located to one side of both endplates, then the component from the distant endplate is the one that is blocked. If the electrode is located between the endplates, then the component that is blocked is the one that corresponds to the wave that fails to reach the electrode first.

The range of IAIs that results in the blocking of a particular MUP component is what we called the component's 'blocking window'. Note that IUI and IAI are both measures of the separation between the discharge times of the two MUPs. They are essentially equivalent, differing only by a constant equal to the inter-endplate propagation time. The IAI cannot be measured directly in an actual EMG signal, whereas the IUI can. The blocking windows for three different electrode locations are shown in Fig. 10*C*. Note that the blocking windows always partition the total blocking range, so that the sum of their widths is always $2t + 2r$. The width of an individual blocking window can range from r to $2t$ + r.

Two points should be noted about the accuracy with which the blocking windows can be measured from EMG signals recorded during voluntary contractions. First, the technique really provides only lower and upper bounds on the window duration (i.e. the largest detected IUI for which blocking did occur and the smallest detected IUI for which it did not occur). The accuracy of the measurement thus depends on the density of the IUI samples. If the two motor units discharge independently of one another, then the IUIs will be distributed randomly and the density will depend on the length of the signal. For example, if both motor units discharge at about 10 Hz, then a signal of 20 s duration will contain about 200 pairs of discharges with IUIs uniformly distributed between −50 and +50 ms. From such a signal, one could expect to estimate the blocking window durations with a resolution of about 0.5 ms.

The second point is that the accuracy of the IUI measurements depends on whether they are based on stable or volatile MUP components. The IUIs in Fig. 8*A* and *B* were based on the occurrence times of the stable components, which accurately reflect the nerve impulse arrival times. The IUIs in Fig. 8*C*, on the other hand, were based on one stable component and one volatile one, and so were less accurate. In particular, the minimum IUI detected beyond the end of the blocking window may have been overestimated.

Absolute refractory period. When the recording site is located to one side of both endplates of a doubly innervated muscle fibre, the width of the shorter blocking window provides an estimate of the absolute refractory period of the fibre (r). In this study, several doubly innervated fibres had blocking windows with widths between 2.1 and 3.7 ms, and none had blocking windows shorter than this. It is probable that the electrode was located to one side of the endplates in many of these cases. Thus the absolute refractory periods of these fibres ranged from 2.1 to 3.7 ms. The range of the absolute refractory period for normal human muscle, determined using the double pulse stimulation technique, has been reported to be 2.2–4.6 ms (Farmer *et al.* 1960) and 2.69–8.13 ms (Mihelin *et al.* 1991). Our estimates fall within the lower portion of this range.

Propagation time between endplates. The propagation time between the two endplates can be estimated by $(w_1 + w_2 - 2r)/2$, where w_1 and w_2 are the lengths of the blocking windows and r is the absolute refractory period. If the recording site is located to one side of both endplates, then this formula reduces to $(w_1 - w_2)/2$, where w_1 is the width of the wider window. We used these formulae to estimate the propagation times between the endplates of each of the doubly innervated fibres. In those instances in which the electrode was clearly located between the endplates, the absolute refractory period was assumed to have a value of 3.0 ms. The estimated propagation times for the doubly innervated fibres depicted in Figs 3, 5 and 7 are shown in the innervation diagrams. The propagation times of all but three of the fibres fell in the range of 7.5 to 11 ms.

Absolute endplate locations. If the recording site is located between the two endplates, then the distances between the endplates and the electrode can be estimated by $l_1 = v(w_1 - r)$ and $l_2 = v(w_2 - r)$, where l_1 and l_2 are the distances, v is the conduction velocity, w_1 and w_2 are the widths of the blocking windows, and r is the absolute refractory period.

Jitter in doubly innervated fibres

Normal MUP waveforms exhibit a small amount of variability in shape from discharge to discharge because of the variability in the relative timing with which the waves of depolarization in the individual fibres reach the electrode. This variability in timing is known as jitter. It has two sources: variability in neuromuscular transmission time, which in normal muscles can contribute between 5 and 60 μs of jitter, and variations in muscle fibre conduction velocity (Stålberg & Trontelj, 1994). Muscle fibre conduction velocity is dependent on the preceding discharge history (Stålberg 1966; Mihelin *et al.* 1991; Stålberg & Trontelj, 1994), and so it fluctuates slightly from discharge to discharge due to the variability of the inter-discharge intervals of the motoneuron. If two muscle fibres from the same motor unit have different conduction velocities, or if their endplates are located at different distances from the electrode, then these fluctuations in conduction velocity will cause a jitter in the arrival times of the waves of depolarization. This is referred to as myogenic jitter, and in normal muscle it is estimated to be less than 10 μs (Stålberg & Trontelj, 1994). Thus in normal muscle, jitter is quite small, and the MUP waveform remains fairly stable from discharge to discharge.

MUPs recorded from motor units containing doubly innervated fibres, on the other hand, can exhibit considerable variability in shape due to a large jitter between the components that are generated by shared and non-shared fibres. Since the shared fibres are activated by more than one motoneuron, their inter-discharge intervals range from just a few milliseconds (when nerve impulses arrive in rapid succession) to the normal motoneuron inter-discharge interval (when blocking occurs). Such large fluctuations result in large fluctuations in conduction velocity. On the other hand, the inter-discharge intervals in the non-shared fibres remain relatively stable, and so do their conduction velocities.

The way in which conduction velocity varies as a function of time after a muscle fibre discharge is known as the velocity recovery function (Stålberg, 1966; Mihelin *et al.* 1991; Stålberg & Trontelj, 1994). Studies using the double

pulse stimulation technique have shown that immediately after the absolute refractory period (i.e. 3 ms after the start of the discharge), conduction velocity is reduced to about 80 % of its normal value. It remains subnormal until about 10 ms and then becomes supernormal, attaining a peak value of about 115 % of its normal value at about 15 ms. It remains substantially above normal until 30 ms, and does not fully return to normal until 1000 ms after the discharge.

The systematic relationships exhibited by the delays of the shared components as shown in Fig. 8 are consistent with the velocity recovery function. The delays were greatest for the shortest inter-unit intervals, when conduction velocity was slowest, and they decreased towards zero at an interval of about 10 ms, when the conduction velocity was no longer subnormal. In some cases, the delay became slightly negative (i.e. the shared component occurred slightly earlier than its normal time) at intervals between 10 and 20 ms, which correspond to the interval of supernormal conduction velocity. However, in general it was not possible to directly estimate the amount by which the conduction velocity had changed since the distance between the endplates and the electrode was not known. This problem was compounded by the fact that the velocity of a wave of depolarization that follows in the wake of a preceding wave of depolarization can vary, becoming slower or faster as it either catches further up or falls further behind. The relatively small delay exhibited by the shared component from a distant endplate (such as d1 in Fig. 8*A*) can be attributed to the fact that the wave of depolarization responsible for the component travels in the opposite direction to the preceding wave, and so encounters the muscle fibre when it has recovered relatively more fully.

Amplitude attenuation in doubly innervated fibres

Associated with the delay, there was a systematic attenuation in amplitude and increase in duration of the components from doubly innervated fibres at short inter-discharge intervals. This is seen most clearly in Fig. 2*C*, traces 9–12, in which the shared fibre discharged in rapid succession (the two discharges are indicated by the circles) and the second component associated with the second discharge was attenuated and broadened as well as delayed. This reflects the known phenomenon that the second intracellular action potential of a pair elicited in rapid succession has a smaller amplitude and a longer rise time than the first (Buchthal & Engbæk, 1963). The difference occurs because the fibre membrane is already slightly depolarized at the beginning of the second action potential due to the negative afterpotential of the first action potential (Buchthal & Engbæk, 1963; Lateva & McGill, 1998). The period of recovery of the action potential amplitude and duration is sometimes referred to as the relative refractory period.

Endplate organization in brachioradialis

The results from this study provide some preliminary insights into the innervation pattern in human brachioradialis. First, they show that the endplates are widely distributed. Of the endplates that we were able to locate with certainty, some were located less than 30 mm distal to the elbow crease while others were more than 90 mm distal to the crease. Second, the results suggest that rather than being distributed randomly, the endplates may be organized in distinct zones. The between-endplate propagation times of almost all the doubly innervated fibres fell within a fairly narrow range, namely 7.5–11 ms. This indicates a consistency of the inter-endplate distances across fibres and across subjects, as would be expected in a zonal organization. The distance between the endplate zones can be calculated, assuming a normal muscle fibre conduction velocity of 3.5–4.0 m s^{-1} (Buchthal & Sten-Knudsen, 1959; Stålberg, 1966), to be between 26 and 44 mm. Moreover, in the one case in which we were able to estimate the relative locations of several endplates at the same time (Fig. 7*A*), they clustered into two spatially separate zones (with the endplates of mn1 and mn3 being in one zone and those of mn2 and mn4 in the other). This is consistent with the finding that the endplates in brachioradialis muscle in stillborn infants were distributed within two zones, one approximately in the middle of the muscle and one more distal (Christensen, 1959).

The results also suggest that the terminal branching of each motoneuron in brachioradialis is confined to a single endplate zone. It has been shown, using transgenic expression of fluorescent proteins, that individual motoneuron axons are capable of branching and forming synapses along the entire length of the spinotrapezius muscle in neonatal mice (Keller-Peck *et al.* 2001). However, if there were motor units in brachioradialis with fractions having endplates 30 mm apart, then we would have expected to see MUPs with components separated by at least 7.5 ms. We did not see any such MUPs.

The results of this study are insufficient to allow estimation of the overall percentage of fibres in brachioradialis that are doubly innervated. Most of the MUP components we recorded behaved as if they came from singly innervated fibres, but this might have been because both co-innervating motoneurons were not active during the recordings. Morphological analysis of the MUP waveforms may reveal more detailed information about motor unit architecture (Lateva & McGill, 2001).

Why are there doubly innervated fibres in brachioradialis?

It is thought that most mammalian skeletal muscles do not have fibres with multiple, widely separated endplates. Those few muscles in which such fibres have been reported all have certain architectural features in common; they are all long, parallel-fibred muscles that contain some short, serially linked fibres (Jarcho *et al.* 1952; Zenker *et al.* 1990; Duxson & Sheard, 1995). The short fibres terminate intrafascicularly, but they are linked in overlapping arrays

to form long fascicles that extend from the origin to the insertion. This serial arrangement of short fibres appears to be a common pattern within long, parallel-fibred muscles in non-primates (Trotter, 1993; Paul, 2001). It allows long muscles to be made up of relatively short individual fibres, which may be advantageous for the excitation–contraction coupling mechanism (Loeb *et al.* 1987; Zenker *et al.* 1990). However, this design also complicates innervation, which is required along the whole muscle length rather than at just a narrow central zone.

The way in which muscles with serially linked fibres develop is illustrated in the embryogenesis of the guinea-pig sternomastoid muscle (Duxson & Sheard, 1995). This is a parallel-fibred muscle that has four distinct endplate zones in both the embryo and the adult. The myotubes in the developing muscle extend from tendon to tendon and are innervated primarily at each of the multiple endplate zones. Each of the points of innervation serves as a focus for the formation of new secondary myotubes, which do not extend the full length of the muscle. It can be extrapolated that the primary myotubes develop into long fibres that retain their multiple innervation, whereas the secondary myotubes develop into short, singly innervated, serially linked fibres.

The ability of supernumerary synapses to coexist on the same muscle fibre appears to depend on their spatial separation. The adjacent endplates on the gunea-pig sternomastoid primary myotubes are separated by 1 to 1.5 mm (Duxson & Sheard, 1995). This is similar to the minimum separation at which experimentally induced ectopic synapses are maintained rather than eliminated in adult rat muscle (Kuffler *et al.* 1977, 1980). Ectopic multiple innervation of normally innervated human brachial triceps muscles by severed ulnar nerves has also been reported (Sunderland, 1952). The signals that mediate the competitive removal of synapses thus evidently operate over only a limited distance.

Human brachioradialis muscle has several similarities with the long, parallel-fibred muscles that exhibit multiple innervation in animals. It has the longest fascicles of any upper limb muscle (Murray *et al.* 2000), with each fascicle extending the length of the muscle from its bony origin at the lateral supracondylar margin of the humerus to its insertion into a long tendon from the styloid process of the distal radius (Feinstein *et al.* 1955; Fridén *et al.* 2001). Although information on individual brachioradialis muscle fibres is limited, one study that employed microdisection and serial cross-sectioning revealed the presence of both long fibres that extend the entire length of the fascicle and short fibres that terminate intrafascicularly (Feinstein *et al.* 1955). The biomechanical function of the brachioradialis muscle is of particular interest in surgical procedures of tendon transfer after nerve or spinal cord injury. Since its function as an elbow flexor is duplicated by other synergistic muscles (brachial biceps and brachialis), brachioradialis is often selected as a donor to replace lost hand function (Fridén *et al.* 2001).

One can speculate that human brachioradialis muscle, like long, parallel-fibred animal muscles, contains both long and short fibres. The multiple endplate zones exist to supply the short fibres, and the long fibres, by chance or by design, receive innervation in more than one endplate zone. There is no reason to believe that this architecture extends to all human muscles, and, indeed, muscles with short fascicles are presumably singly innervated according to the classical model. However, there may be other long-fascicled human muscles in addition to brachioradialis which do also contain long fibres with multiple, widely separated endplates. One possibility is brachial biceps, which has been suggested to contain multiply innervated fibres on the basis of collision studies (McComas *et al.* 1984). However, we have never observed the types of discharge and waveform irregularities in brachial biceps that would indicate polyneuronal innervation. Other possibilities include the sartorius and gracilis muscles in the thigh (Heron & Richmond, 1993) and the latissimus dorsi muscle in the back (Snobl *et al.* 1998).

Implications for motor control

At present, the physiological purpose of muscle fibres with multiple endplates and polyneuronal innervation remains largely unknown. They may not serve any important purpose at all, being merely an artifact of development, limited to a small percentage of fibres and having only an inconsequential effect on the overall functioning of the muscle. Our preliminary observations do not support the idea that the nervous system uses any special mechanism to co-ordinate the co-activation of doubly innervated fibres at the individual fibre level. We noticed no especially high degree of synchronization between the discharge patterns of co-innervating motoneurons. Furthermore, the example in Fig. 7 shows that the same motoneuron can be involved in co-innervation relationships with more than one other motoneuron. It does not seem possible that the co-activation of every shared fibre could be co-ordinated effectively given such a complicated arrangement of co-innervation.

On the other hand, a scaffold of long fibres may play an essential role in transmitting forces generated by short, serially linked fibres, and polyneuronal innervation may provide an effective way for the nervous system to activate muscles with this architecture. The short fibres, being singly innervated, receive excitation at the discharge rate of the innervating motoneuron. The long fibres, being polyneuronally innervated, receive excitation at a rate that approaches the sum of the discharge rates of the co-innervating motoneurons. This may serve to maintain fused, tetanic contractions in the long fibres even during

fairly weak contractions of the overall muscle. Furthermore, tetanic excitation of long fibres may also serve to mitigate the difficulties associated with the inability to excite their entire lengths simultaneously during individual twitches.

REFERENCES

Aquilonius, S. M., Askmark, H., Gillberg, P. G., Nandedkar, S., Olsson, Y. & Stålberg, E. (1984). Topographical localization of motor endplates in cryosections of whole human muscles. *Muscle and Nerve* **7**, 287–293.

Brown, M. C. & Matthews, P. B. C. (1960). An investigation into possible existence of polyneuronal innervation of individual skeletal muscle fibres in certain hind-limb muscles of the cat. *Journal of Physiology* **151**, 436–457.

Buchthal, F. & Engbæk, L. (1963). Refractory period and conduction velocity of the striated muscle fibre. *Acta Physiologica Scandinavica* **59**, 199–220.

Buchthal, F. & Sten-Knudsen, O. (1959). Impulse propagation in striated muscle fibres and the role of the internal currents in activation. *Annals of the New York Academy of Sciences* **81**, 422–445.

Christensen, E. (1959). Topography of terminal motor innervation in striated muscles from stillborn infants. *American Journal of Physical Medicine* **38**, 65–78.

Coërs, C. & Woolf, A. L. (1959). *The Innervation of Muscle: a Biopsy Study*. Blackwell, Oxford.

Costanzo, E. M., Barry, J. A. & Ribchester, R. R. (2000). Competition at silent synapses in reinnervated skeletal muscle. *Nature Neuroscience* **3**, 694–700.

Desmedt, J. E. (1958). Méthodes d'étude de la fonction neuromusculaire chez l'Homme. *Acta Neurologica Belgica* **58**, 977–1017.

Duxson, M. J. & Sheard, P. W. (1995). Formation of new myotubes occurs exclusively at the multiple innervation zones of an embryonic large muscle. *Developmental Dynamics* **204**, 391–405.

Farmer, T. W., Buchthal, F. & Rosenfalck, P. (1960). Refractory period of human muscle after the passage of a propagated action potential. *Electroencephalography and Clinical Neurophysiology* **12**, 455–466.

Feinstein, B., Lindegard, B., Nyman, E. & Wohlfart, G. (1955). Morphological studies of human muscles. *Acta Anatomica* **23**, 127–142.

Fridén, J., Albrecht, D. & Lieber, R. L. (2001). Biomechanical analysis of the brachioradialis as a donor in tendon transfer. *Clinical Orthopaedics and Related Research* **383**, 152–161.

Happak, W., Liu, J., Burggasser, G., Flowers, A., Gruber, H. & Freilinger, G. (1997). Human facial muscles: dimensions, motor endplate distribution, and presence of muscle fibres with multiple motor endplates. *Anatomical Record* **249**, 276–284.

Heron, M. I. & Richmond, F. J. R. (1993). In-series fibre architecture in long human muscles. *Journal of Morphology* **216**, 35–45.

Hunt, C. C. & Kuffler, S. W. (1954). Motor innervation of skeletal muscle: multiple innervation of individual muscle fibres and motor function. *Journal of Physiology* **126**, 293–303.

Jarcho, L. W., Eyzaguirre, C., Berman, B. & Lilienthal, J. L. Jr (1952). Spread of excitation in skeletal muscle: some factors contributing to the form of the electromyogram. *Journal of Physiology* **168**, 446–457.

Katz, B. & Kuffler, S. W. (1941). Multiple motor innervation of the frog's sartorius muscle. *Journal of Neurophysiology* **4**, 209–223.

Keller-Peck, C. R., Walsh, M. K., Gan, W. B., Feng, G., Sanes, J. R. & Lichman, J. W. (2001). Asynchronous synapse elimination in neonatal motor units: studies using GFP transgenic mice. *Neuron* **31**, 381–394.

Kuffler, D., Thompson, W. & Jansen, J. K. (1977). The elimination of synapses in multiply-innervated skeletal muscle fibres of the rat: dependence on distance between end-plates. *Brain Research* **138**, 353–358.

Kuffler, D., Thompson, W. & Jansen, J. K. (1980). The fate of foreign endplates in cross innervated rat soleus muscle. *Proceedings of the Royal Society* B **177**, 189–222.

Lateva, Z. C. & McGill, K. C. (1998). The physiological origin of the slow afterwave in muscle action potentials. *Electroencephalography and Clinical Neurophysiology* **109**, 462–469.

Lateva, Z. C. & McGill, K. C. (2001). Estimating motor-unit architectural properties by analysing motor-unit action potential morphology. *Clinical Neurophysiology* **112**, 127–135.

Loeb, G. E., Pratt, C. A., Chanaud, C. M. & Richmond, F. J. R. (1987). Distribution and innervation of short, interdigitated muscle fibres in parallel-fibered muscles of the cat hindlimb. *Journal of Morphology* **191**, 1–15.

McComas A. J., Kereshi, S. & Manzano, G. (1984). Multiple innervation of human muscle fibres. *Journal of the Neurological Sciences* **64**, 55–64.

McGill, K. C. (2002). Optimal resolution of superimposed action potentials. *IEEE Transactions on Biomedical Engineering* **49**, 640–650.

McGill, K. C. & Dorfman L. J. (1984). High-resolution alignment of sampled waveforms. *IEEE Transactions on Biomedical Engineering* **31**, 462–468.

Merton, P. A. (1954). Interaction between muscle fibres in a twitch. *Journal of Physiology* **124**, 311–324.

Mihelin, M., Trontelj, J. V. & Stålberg, E. (1991). Muscle fibre recovery functions studied with double pulse stimulation. *Muscle and Nerve* **14**, 739–747.

Murray, W. M., Buchanan, T. S. & Delp, S. L. (2000). The isometric functional capacity of muscles that cross the elbow. *Journal of Biomechanics* **33**, 943–952.

Navarrete, R. & Vrbova, G. (1993). Activity-dependent interactions between motoneurones and muscles: their role in the development of the motor unit. *Progress in Neurobiology* **41**, 93–124.

Paul, A. C. (2001). Muscle length affects the architecture and pattern of innervation differently in leg muscles of mouse, guinea pig, and rabbit compared to those of human and monkey muscles. *Anatomical Record* **262**, 301–309.

Perie, S., St Guily, J. L., Callard, P. & Sebille, A. (1997). Innervation of adult human laryngeal muscle fibres. *Journal of Neurological Sciences* **149**, 81–86.

Personius, K. E. & Balice-Gordon, R. J. (2001). Loss of correlated motor neuron activity during synaptic competition at developing neuromuscular synapses. *Neuron* **31**, 395–408.

Rossi, G. (1990). From the pattern of human vocal muscle fibre innervation to functional remarks. *Acta Otolaryngologica* **473**, 1–10.

Sandmann, G. (1885). Ueber die Vertheilung der motorischen Nervenendapparate in den quergestreiften Muskeln der Wirbelthiere. *Archiv für Anatomie und Physiologie* (Leipzig), 240–252.

Sanes, J. S. & Lichman, J. W. (1999). Development of the vertebrate neuromuscular junction. *Annual Review of Neuroscience* **22**, 389–442.

Sheard, P. W., McHannigan, P. & Duxson, M. J. (1999). Single and paired motor unit performance in skeletal muscles: comparison between simple and series-fibred muscles from the rat and the guinea pig. *Basic Applied Myology* **9**, 79–87.

Sherrington, C. S. (1930). Some functional problems attaching to convergence. *Proceedings of the Royal Society* B **105**, 332–362.

Snobl, D., Binaghi, L. E. & Zenker, W. (1998). Microarchitecture and innervation of the human latissimus dorsi muscle. *Journal of Reconstructive Microsurgery* **14**, 171–177.

Stålberg, E. (1966). Propagation velocity in human muscle fibres in situ. *Acta Physiologica Scandinavica* **70** (suppl. 287), 1–112.

Stålberg, E. & Trontelj, J. V. (1994). *Single Fibre Electromyography in Healthy and Diseased Muscle.* Raven Press, New York.

Sunderland, S. (1952). The multiple motor innervation of individual muscle fibres in man. *Acta Anatomica* **16**, 167–168.

Troiani, D., Filippi, G. M. & Bassi, F. A. (1999). Nonlinear tension summation of different combinations of motor units in the anesthetized cat peroneus longus muscle. *Journal of Neurophysiology* **81**, 771–780.

Trotter, J. A. (1993). Functional morphology of force transmission in skeletal muscle. *Acta Anatomica* **146**, 205–222.

Trotter, J. A., Richmond, F. J. & Purslow, P. P. (1995). Functional morphology and motor control of series-fibered muscles. *Exercise and Sport Sciences Reviews* **23**, 167–213.

Vrbova, G., Gordon T. & Jones, R. (1995). *Nerve-Muscle Interaction.* Chapman & Hall, London.

Zenker, W., Snobl, D. & Boetschi, R. (1990). Multifocal innervation and muscle length. A morphological study on the role of myo-myonal junctions, fibre branching and multiple innervation in muscles of different size and shape. *Anatomy and Embryology* **182**, 273–283.

Acknowledgements

This work was supported by the Medical and Rehabilitation Research and Development Services of the US Department of Veterans Affairs.